Transfer of modified fecal viromes alleviates symptoms of non-alcoholic liver disease and improve blood glucose regulation in an obesity mouse model

Xiaotian Mao[1], Sabina Birgitte Larsen[1], Line Sidsel Fisker Zachariassen[2], Anders Brunse[3], Signe Adamberg[4], Josue Leonardo Castro Mejia[1], Kaarel Adamberg[4,5], Dennis Sandris Nielsen[1], Axel Kornerup Hansen[2], Camilla Hartmann Friis Hansen[2], Torben Sølbeck Rasmussen[1*]

Author affiliations

1 Section of Microbiology and Fermentation, Dept. of Food Science, University of Copenhagen, Frederiksberg, Denmark

2 Section of Experimental Animal Models, Dept. of Veterinary and Animal Sciences, University of Copenhagen, Frederiksberg, Denmark

3 Section of Comparative Pediatrics and Nutrition, Dept. of Veterinary and Animal Sciences, University of Copenhagen, Frederiksberg, Denmark

4 Department of Chemistry and Biotechnology, Tallinn University of Technology, Tallinn, Estonia

5 Center of Food and Fermentation Technologies, Tallinn, Estonia

**Address correspondence to torben@food.ku.dk (+45 35 32 80 73), Rolighedsvej 26 4th floor, 1958 Frederiksberg C, Denmark.*

Keywords: Fecal virome transplantation, gut microbiome, type-2 diabetes, NAFLD, phage therapy, obesity

Abstract

Metabolic syndrome encompasses amongst other conditions like obesity, type-2 diabetes, and non-alcoholic fatty liver disease, that all are associated with gut microbiome (GM) dysbiosis. Fecal microbiota transplantation (FMT) has been explored to treat metabolic syndrome by restoring the GM. FMT is generally safe, but motivated by case-reports, accidental transfer of pathogenic bacteria remains a concern. Fecal virome transplantation (FVT, sterile-filtrated feces) from lean donors has shown promise in alleviating metabolic effects of a high-fat diet. FVT has the advantage over FMT that mainly bacteriophages are transferred but still carries the risk of eukaryotic viral infections. To address this, modified FVTs were compared with unmodified FVT and saline in a mouse model of diet-induced obesity. Unmodified-FVT improved liver pathology and reduced adipose inflammation, while "eukaryotic-virus-free" FVT enhanced blood glucose clearance. GM analysis suggested bacteriophage-mediated GM modulation had influenced these outcomes. This may pave the way for developing bacteriophage-based therapies for metabolic syndrome through GM restoration.

Introduction

Obesity is a severe metabolic disease that affects millions worldwide due to high-calorie foods and a sedentary lifestyle[1]. It is also a risk factor for the later development of other metabolic comorbidities, such as type-2 diabetes and non-alcoholic fatty liver disease (NAFLD)[2,3]. While many patients with obesity can achieve significant weight loss, only a few can maintain their long-term body weight. It is increasingly recognized that a dysbiotic gut microbiome (GM) plays a crucial role in the persistence of obesity[2]. Therefore, targeting the GM for the treatment of metabolic syndrome and restoring its balance is an attracting approach. Fecal microbiota transplantation (FMT) has shown high treatment efficacy in targeting recurrent *Clostridioides difficile* infections (rCDI)[4], as well as a potential importance in colorectal cancer treatments[5], and the prevention of necrotizing enterocolitis[6,7]. FMT has also been investigated to alleviate symptoms of metabolic syndrome[8–10]. Although some positive effects have been reported when using FMT to treat patients suffering from obesity and type-2 diabetes[8–10], these effects are usually limited and short-term. Despite the high success rates in treating rCDI[4] and the rigorous donor screening, FMT remains a last resort for patients who do not respond to antibiotics due to safety concerns[11]. The reasoning of this caution was exemplified by the death of a patient in 2019 due to a bacterial infection following FMT[12], as well as subsequent safety alerts from authorities[13,14]. Consequently, while FMT has the potential to revolutionize treatments for numerous gut-related diseases, its widespread use seems unlikely due to these inherent safety issues of transferring pathogenic microorganisms. The fecal matrix of FMT includes bacteria, archaea, eukaryotes, viruses, and gut metabolites, which may be responsible for both the beneficial and detrimental effects of FMT[15]. Therefore, reducing the complexity of the donor fecal matrix while maintaining its therapeutic efficacy would improve safety in clinical settings.

The gut virome is thought to play a key role in shaping and maintaining the composition of the GM and host metabolism[16,17]. It mainly consists of bacteriophages (phages), which are viruses that infect bacteria in a host-specific manner[18], while archaeal and eukaryotic viruses constitute the remaining. Screening assays can be used to detect known pathogenic viruses before performing FMT. However, in recent years, it has become evident that the human gastrointestinal tract harbors hundreds of eukaryotic viruses with unknown functions[17,19,20]. Although most of these viruses are likely harmless, their potential role in later disease development should not be overlooked, as seen for the human papillomavirus that can induce cervical cancer years after infection[21].

Independent studies have successfully treated patients suffering from rCDI with sterile filtrated donor feces (containing mainly viruses and no bacteria) which were shown to be as effective as FMT[4,22,23]. This approach is often referred to as fecal virome transplantation (FVT). In preclinical settings, FVT has also been shown to alleviate symptoms of type-2 diabetes and obesity[24,25], as well as prevent the onset of necrotizing enterocolitis in preterm piglets[6]. FVT has an advantage over FMT in that it transfers no or very few bacteria. However, the centrifugation and filtration steps used in preparing FVT cannot separate phages from eukaryotic viruses due to their similar sizes.

In two recent studies, we aimed to enhance the safety of FVT by developing methodologies that selectively inactivate[26] or remove the eukaryotic viruses from the fecal matrix[27] while preserving an active gut phage community. To achieve this, we utilized the differences in key characteristics between eukaryotic viruses and phages[26,27]; most eukaryotic viruses are enveloped RNA viruses[28,29] that only infect eukaryotic cells and most phages are non-enveloped DNA viruses[29,30] infecting only bacteria. Solvent/detergent treatment (approved by the World Health Organization for treating blood plasma[31]) was used to inactivate enveloped viruses[32] (FVT-SDT), a compound (pyronin Y) that specifically binds to RNA[33,34] was applied to inactivate RNA viruses (FVT-PyT), and an optimized chemostat fermentation of fecal inoculum aimed at removing the eukaryotic viruses by dilution[27] (FVT-ChP). We demonstrated that FVT-SDT and FVT-ChP showed promising results in treating *C. difficile* infections in a mouse model[26], which represents a simple disease etiology mainly caused by the toxin-producing *C. difficile*[35].

As a follow-up study, we here hypothesize that the same modified FVTs maintain their alleviating effects of FVT on symptoms associated with metabolic syndrome that we previously have shown[24]. A diet-induced obesity model[36] is used a proof-of-concept since it represents a more complex GM-associated disease compared to a simple *C. difficile* infection model[26].

Results

Improved clearance of blood glucose and alleviated symptoms of NAFLD following FVT

Oral glucose tolerance tests (OGTT) of the mice were performed after 13 weeks (18 weeks old, Fig. S1A and S1B) and 18 weeks (23 weeks old, Fig. 1C & 1D) on their respective diets to evaluate their blood glucose regulation. At study week 18 (23 weeks old), mice on a high-fat diet had significantly ($p < 0.05$) elevated fasting blood glucose levels and impaired glucose

regulation during the first 15 minutes after administration compared with lean controls (Fig. 1D). Blood glucose levels of mice treated with the chemostat propagated virome (FVT-ChP) decreased sharply from 30 min to 60 min after glucose administration (Fig. 1D). This highlighted a significantly ($p < 0.05$) improved blood sugar regulation of the FVT-ChP treated mice, compared with the obese control (Fig. 1C). No FVT treatments significantly improved OGTT scores at the 13 weeks measure (Fig. S1A & S1B). A NAFLD activity score was determined by liver histopathology (Fig. 1E & S1C). Mice treated with unmodified FVT had a significantly ($p < 0.05$) lower NALFD activity score compared to obese controls. FVT-ChP, FVT-SDT, and FVT-PyT treated mice scored significantly higher ($p < 0.05$) than lean controls but similarly to obese controls (Fig. 1E). Weight gain was measured to assess the impact of different treatments on body weight. The obese control mice showed a significant increase ($p < 0.05$) in body weight, epididymal white adipose tissue (eWAT), and blood glucose levels compared to lean controls at the termination of the study (23 weeks old) (Fig. 1A, 1B, & 1C), confirming the expected progression of the diet-induced obesity model. Body weight and eWAT size was not improved by any of the FVT treatments compared to obese controls at termination (Fig. 1A and 1B).

Unmodified fecal virome alleviated pro-inflammatory immune response in adipose tissue

Flow cytometry was performed to evaluate the presence of immune cells in eWAT (Fig. 2A-L) at termination (23 weeks old). Interestingly, mice treated with the unmodified FVT showed a decrease in the proportions of central memory CD8+ T cells (CD44+CD62l+) ($p < 0.05$), dendritic cells ($p < 0.05$), and M1 macrophages ($p < 0.05$) compared to obese controls (Fig. 2A, 2C, & 2G). Hence, this signal of alleviated adipose inflammation supported the improvement of liver histopathology (Fig. 1E). Except for mice treated with unmodified FVT, mice fed a high-fat diet generally appeared with a significant ($p < 0.05$) increase in the level of dendritic cells (% CD11c+ of all CD45+ leukocytes), CD8+ T cells, CD19+ B cells, and in the proportion of macrophages with a proinflammatory M1 phenotype (% CD11c+ of F4.80+ macrophages), when compared with the lean control group (Fig. 2). Immune cells in the mesenteric lymph node (MLN) were also counted but showed no clear differences between treatment groups (Fig. S2).

Undesirable inflammatory response associated with the chemostat-propagated virome

Motivated by the observed effects on OGTT and histological measures, we examined the cytokine profile of mouse blood serum. The overall cytokine profile of serum from mice treated

with unmodified FVT was not different from that of obese control mice. Therefore, the cytokine profile does not explain the improved liver pathology (Fig. 1E). In contrast, the serum cytokine profile of FVT-ChP treated mice showed significantly elevated ($p < 0.05$) expression of several pro-inflammatory cytokines, including IL-15, TNF-α, and MIP-2, compared to the cytokine profiles of unmodified FVT-treated, obese, and lean control mice (Fig. 3). This indicated an undesirable increase in systemic inflammation associated with the FVT-ChP treatment. However, the flow cytometry analysis did not detect immune cell levels reflecting inflammation in the adipose tissue of FVT-ChP treated mice.

Transplantation of modified fecal viromes shifted the gut microbiome composition

The gut bacterial and viral composition of the mice were investigated at three time points: upon arrival at our housing facilities (5 weeks old), 1 week after the 2nd FVT (14 weeks old), and at termination (23 weeks old). At the end of the study, both the FVT-ChP and unmodified FVT treated mice had significantly ($p < 0.05$) altered their gut bacterial composition (Bray-Curtis dissimilarity) compared to the obese control group (Fig. 4 & Table S1). The dominant bacterial phyla detected in the mice feces were *Firmicutes*, *Bacteroidetes*, *Actinobacteria*, *Proteobacteria*, *Deferribacteres*, and *Verrucomicrobia* (Fig. S3I & S3J). The relative abundance of the bacterial genus *Allobaculum* was significantly higher in both the FVT-ChP treated mice ($p < 0.05$) and the lean control group ($p < 0.005$) compared to the obese control mice at the end of the study (Fig. S3A). The bacterial GM profile of the FVT-ChP treated mice was particularly characterized by a significantly ($p < 0.05$) increased relative abundance of lactobacilli compared to all other groups (Fig. S3F). The bacterial composition of all mice upon arrival at our housing facility appeared similar based on bacterial diversity (Shannon diversity index) and bacterial composition (Fig. 4A & 4B).

None of the FVT treatments affected gut viral diversity. However, the viral composition of mice treated with unmodified FVT, FVT-ChP, and FVT-SDT was all significantly ($p < 0.05$) different compared to the obese control (Fig. 5A, 5B, & Table S2). Differential viral abundance was analyzed at the level of viral contigs (vOTUs) and their predicted bacterial hosts (Fig. S4 & S5) to elucidate potential host-phage interactions. When comparing both FVT-ChP and unmodified FVT treated mice to the obese control at the end of the study, significant ($p < 0.05$) differences were observed in the relative abundance of viruses belonging to the family *Microviridae* and order *Caudovirales* (Fig. S4), as well as viruses with predicted bacterial hosts belonging to the genera *Parabacteroides*, *Bacteroides*, *Prevotella*, and *Akkermansia* (Fig. S5).

This suggests that the transfer of modified or unmodified fecal virome had an impact on the viral gut component of the mice over 18 weeks. The taxonomic profiles of the applied fecal viromes were also dominated by *Microviridae* and *Caudovirales*-associated viruses. Eukaryotic viruses appeared to be significantly depleted in the FVT-ChP inoculum in terms of relative abundance (0.015%) compared to the FVT-SDT (1.82%), unmodified FVT (0.61%), and FVT-PyT (1.75%) inoculum (Fig. S6E).

Discussion

Here, we address the safety considerations associated with the risk of infections by eukaryotic viruses when using fecal virome transplantation (FVT) for treating diseases associated with gut dysbiosis. We apply recently developed methodologies to either inactivate or remove the eukaryotic component of FVT while maintaining an active enteric phage community[26,27]. The potential of these modified FVTs to alleviate symptoms of metabolic syndrome was investigated using a diet-induced obesity mouse model.

Previously we have shown that unmodified FVT could reduce weight gain and normalize blood glucose regulation[24]. We could only partly replicate these results in the current study since no clear differences in weight gain and eWAT size were observed when comparing any of the FVT treatment groups with the obese control mice. Additionally, the unmodified FVT did not show a significant improvement of the blood glucose regulation as previously demonstrated[24]. These discrepancies are likely explained by differences in the GM of the donor materials[37] which can vary between mouse vendor facilities and pose challenges to reproducibility[38–41]. Instead, mice treated with a chemostat-propagated virome (FVT-ChP) expressed improved blood glucose regulation compared with the obese control. Considering the reported reproducibility of chemostat propagated enteric phageomes[27,42] (inoculated with either mouse or human inoculum), this approach may open interesting perspectives for enhancing the reproducibility of FVT-based studies and significantly reducing the number of eukaryotic viruses transferred.

Liver histopathology was performed to assess the NADFL activity since the liver is involved in important metabolic functions[24,43]. The high-fat diet had induced NAFLD-like manifestations in the liver tissue as expected in the obese control mice, however, the mice treated with unmodified FVT expressed a significantly improved NAFDL activity score. This may be in line with an earlier study[24], where unmodified FVT showed capable to affect the

expression of genes with important metabolic functions to be more like the lean control than the obese control mice.

The inflammatory state of obesity is associated with an accumulation of macrophages in the adipose tissue[44], where the activated macrophages are recruited by $CD8^+$ T cells[45]. Additionally, elevated levels of dendritic cells can play a role in the immune response to liver injury[46]. In this study, reductions in the number of CD8+ T cells, activated macrophages, and dendritic cells were observed in the mice treated with unmodified FVT compared to the obese control, suggesting that unmodified FVT had alleviated adipose inflammation in the mice, which may be linked to the observed reduction in liver pathology.

The cytokine profile of the mouse blood serum was examined since low-grade systemic inflammation is linked to metabolic syndrome[47,48]. Especially elevated levels of the cytokines MIP-2, IL-15, and TNF-α in the FVT-ChP treated mice indicated increased inflammation. The recruitment and activation of neutrophils via MIP-2 can prompt the release of diverse inflammatory mediators, which can hasten the onset of liver inflammation[49]. TNF-α is produced by adipose tissue and works as a pro-inflammatory cytokine that has been shown to play a role in the development of NAFLD[50,51]. Overexpression of IL-15 in transgenic mice and IL-15 treatment of NOD mice have been reported to improve glucose tolerance[52]. As a double edge sword, the increased levels of pro-inflammatory cytokines (MIP-2, IL-15, and TNF-α) in the blood serum of FVT-ChP treated mice compared to the obese control may partly explain their improved blood glucose regulation as well as the lack of improvement in their associated histopathology liver score compared to the obese control mice.

A significant increase in the relative abundance of *Allobaculum* was detected in feces samples from the FVT-ChP treated mice compared with the obese control ($p < 0.05$) and unmodified FVT ($p < 0.005$), while not being different from the relative abundance of *Allobaculum* in the lean control mice (Fig. S3A). *Allobaculum* is a Gram-negative bacteria found in both murine and human hosts[53,54]. *Allobaculum* is linked with improved insulin response in high-fat diet-induced metabolic syndrome[55,56], which supports our observations of improved blood glucose regulation in the FVT-ChP treated mice. Elevated levels of lactobacilli in patients suffering from non-alcoholic fatty liver disease (NAFLD) have been reported[57,58]. A higher relative abundance of lactobacilli in FVT-ChP-treated mice compared with all other groups could therefore be involved with the increased pro-inflammatory response and NAFDL symptoms. Differences in etiology may explain our findings of improved blood glucose control in FVT-

ChP treated mice and reduced NAFLD symptoms in mice treated with unmodified FVT. Determination of differentially abundant viral contigs (vOTUs) and their predicted bacterial hosts showed clear differences when comparing the FVT-ChP treatment with the unmodified FVT (Fig. S4 & S5). Hence, these differences in viral profiles may have contributed to the two different phenotypes.

Most of the drug-based treatments for chronic diseases are long-term or periodic[59], but this study only treated mice with FVT twice. Compared with the phenotypical changes induced by a long-term high-fat diet, two FVT treatments may be insufficient, raising the question if the number and frequency of FVT treatments should be adjusted in future intervention studies. To summarize, it was possible to maintain the alleviating effects of FVT[24] on metabolic syndrome-associated symptoms with a reproducible chemostat-propagated enteric virome that was depleted for eukaryotic viruses. While the unmodified FVT showed the most substantial phenotypic improvement in terms of reducing diet-induced damage of liver tissue and lowered adipose inflammation. The elements driving the improved liver histopathology in the unmodified FVT may be lost during the chemostat fermentation of donor feces, which calls for further refinement of the chemostat propagation of viromes as a therapeutic tool targeting diseases associated with gut dysbiosis.

Methods

The animal origin and preparation of donor viromes

A total of 54 male C57BL/6N mice were purchased for the purpose of harvesting intestinal content for downstream FVT applications. Upon arrival, the mice were five weeks old and obtained from three vendors: 18 C57BL/6NTac from Taconic (Denmark), 18 C57BL/6NRj from Janvier (France), and 18 C57BL/6NCrl from Charles River (Germany). The mice were earmarked upon arrival, randomly assigned according to vendor to 3 cages with 6 mice each, and housed at the Section of Experimental Animal Models, University of Copenhagen, Denmark, following previously described conditions[41]. They were provided with ad libitum access to a low-fat diet (LF, Research Diets D12450J) for a period of 13 weeks until they reached 18 weeks of age, which was the planned termination point. Unfortunately, malocclusions resulted in malnutrition for two C57BL/6NRj mice, and they were euthanized before the intended termination date. All mice were euthanized by cervical dislocation, and samples of intestinal content from the cecum and colon were collected and suspended in 500µL of autoclaved anoxic PBS buffer (NaCl 137mM, KCl 2.7mM, Na_2HPO_4 10mM, KH_2PO_4

1.8mM). Subsequently, all samples were stored at -80°C. In order to preserve the viability of strict anaerobic bacteria, 6 mice from each vendor (a total of 18 mice) were sacrificed and immediately transferred to an anaerobic chamber (Coy Laboratory) containing an atmosphere of approximately 93% N_2, 2% H_2, and 5% CO_2, maintained at room temperature. The samples collected from these mice within the anaerobic chamber were used for anaerobic chemostat cultivation to produce the chemostat propagated virome (FVT-ChP). The intestinal content from the remaining 34 mice was sampled under aerobic conditions and used to generate the fecal virome for downstream processing of the FVT-UnT, FVT-SDT, and FVT-PyT treatments. A flow diagram illustrating the aforementioned processes is provided (Fig. S7). All procedures for handling animals used for collecting donor material were carried out in accordance with the Directive 2010/63/EU and the Danish Animal Experimentation Act with the license ID: 2012-15-2934-00256.

Unmodified fecal virome

Intestinal content from cecum and colon was thawed and processed to produce FVT solutions as previously described[24], with the exception of Centriprep Ultracel YM-50K units (Millipore) being replaced with YM-30K units, which is applied to concentrate fecal viromes and remove metabolites below the size of 30 kDa. Fecal viromes of mice from all vendors were mixed and divided into three aliquots. One was immediately stored at -80°C and represented the unmodified FVT. The two-remaining fecal virome aliquots were further processed for inactivation of eukaryotic viruses by either dissolving the lipid membrane of enveloped viruses with solvent/detergent treatment or inhibiting replication of RNA viruses with pyronin Y treatment.

Solvent/detergent-treated fecal virome (FVT-SDT)

The solvent/detergent treatment is commonly used for inactivating enveloped viruses (most eukaryotic viruses are enveloped) in blood plasma, while non-enveloped viruses (most phages are non-enveloped) are not inactivated[32,60,61]. The fecal viromes were treated according to the recommendations from the WHO for clinical use of solvent/detergent treated plasma; incubation in 1% (w/v) tri(n-butyl) phosphate (TnBP) and 1% (w/v) Triton X-100 at 30°C for 4 hours[31]. Solvent/detergent treatment was performed by following the method of Horowitz *et al.*[32] and the removal of TnBP and Triton X-100 was performed as described by Treščec *et al.*[62]. The removal of the solvent/detergent agents from the fecal virome yielded approx. 100 mL viral-flow-through from the column, which was concentrated to 0.5 mL using Centriprep Ultracel YM-30K units. The final product constituted the FVT-SDT treatment.

Pyronin Y treated fecal virome (FVT-PyT)

Pyronin Y (Merck) is a strong red-colored fluorescent compound. It has been reported to exhibit efficient binding to single-stranded and double-stranded RNA (ss/dsRNA), while its binding to single-stranded and double-stranded DNA (ss/dsDNA) is less effective[33,34]. The fecal filtrate was treated with 100µM pyronin Y and incubated at 40°C overnight to inactivate viral particles containing RNA genomes[26]. To remove the pyronin Y molecules that were not bound, the pyronin Y treated fecal filtrate suspensions were diluted in 50mL SM buffer and subsequently concentrated to 0.5mL using Centriprep Ultracel YM-30K units. This process was repeated three times, resulting in a transparent appearance of the pyronin Y treated fecal filtrate, which constituted the FVT-PyT treatment.

Chemostat propagated fecal virome (FVT-ChP)

The preparation of the chemostat propagated virome was performed as described in another study[27]. In brief, anoxic-handled cecum content from mice was used as inoculum for chemostat propagation. The culture medium was designed to mimic the low-fat diet (Research Diets D12450J) that was provided to the lean donor mice, and the growth conditions as temperature, pH, etc., were set to mimic the environmental conditions found in mouse cecum. The end cultures fermented with a slow dilution rate (0.05 volumes 1/h, simulating transit time) showed to generate a microbial composition closest to the donor's initial microbial composition profile[27], and these three batches were mixed and constituted the FVT-ChP treatment.

Fluorescence microscopy

Virus-like particle (VLP) counts were evaluated of all applied fecal viromes (unmodified FVT, FVT-SDT, FVT-ChP, and FVT-PyT) by epifluorescence microscopy stained by SYBR™ Gold (Thermo Scientific, cat. no. S11494) as described dx.doi.org/10.17504/protocols.io.bx6cpraw. The viral concentration was normalized to 2 x 10^9 VLP/mL per treatment.

Animal model design of diet-induced obesity

Forty-eight male C57BL/6NTac mice (Taconic Biosciences A/S, Lille Skensved, Denmark) were divided randomly into 6 groups at 5 weeks old: lean control, obese control, unmodified FVT (as the control for modified FVTs), FVT-ChP, FVT-SDT, and FVT-PyT (Fig. 6). Only male C57BL/6NTac mice were included since female mice are protected against diet-induced obesity[63]. For 18 weeks, mice were fed ad libitum high-fat diet (Research Diets D12492), except lean controls that were fed a low-fat diet (Research Diets D12450J). After 6 weeks on their respective diets, mice were administered 0.15 mL of the unmodified FVT, FVT-ChP,

FVT-SDT, or FVT-PyT by oral gavage twice with one week of interval (study weeks 7 and 8). Obese and lean controls received 0.15 mL SM buffer as sham through oral gavage. The titre of the applied FVT virome was approximately 2×10^9 VLP/mL (Fig. S6A-D). The mice were subjected to an oral glucose tolerance test (OGTT) at week 13 and 18 of the study (18 and 23 weeks old) by blinded personnel, and food intake and mouse weight were monitored frequently. OGTT outliers were removed if 2 of 3 parameters were applicable: 1) tAUC > 2000 mg/dL, fasting glucose > 11.5 mM, or 3) loss of 5-10% in body weight. Blood serum, eWAT, MLN, liver tissue, intestinal content from the cecum and colon, and tissue from the colon and ileum were sampled at termination at study week 18 (23 weeks old) and stored at -80ºC until downstream analysis. Liver tissue was fixated in 10% neutral-buffered formalin (Sarstedt Formalin System) for histological analysis and stored at room temperature until further processed. All procedures regarding the handling of animals included in the diet-induced obesity model were carried out in accordance with the Directive 2010/63/EU and the Danish Animal Experimentation Act with the license ID: 2017-15-0201-01262 C1, and the and housing and enrichment conditions were as earlier described[41].

Cytokine analysis

Serum samples were diluted 1:2 and analyzed for IFN-γ, GM-CSF, IL-15, IL-6, IL-10, KC/GRO, MIP-2, and TNF-α IL-17A/F, and IL-22 in a customized metabolic group 1 U-PLEX (Meso Scale Discovery, Rockville, ML) according to manufacturer's instructions. Concentrations were extrapolated from a standard curve, and measurements out of detection range were assigned the value of lower or upper detection limit.

Histology

Formalin-fixed liver biopsies were embedded in paraffin, sectioned, and stained with hematoxylin & eosin for histopathological evaluation. We used a cumulative semi-quantitative NAFLD activity score (NAS) comprising the following three histological features: Steatosis (0-3), immune cell margination and infiltration (0-2), and hepatocellular ballooning (0-2) with higher values corresponding to increased dissemination. The histological assessment was performed by a blinded investigator (Co-author AB).

Cell isolation and flow cytometry

Directly after sacrificing the mice, the MLN and eWAT were placed in ice cold PBS. Single-cell suspensions were prepared by disrupting the lymph node between two microscope glasses and passing it through a 70 µm nylon mesh. eWAT cells were isolated as previously

described[64]. After washing in PBS and resuspension, 1 x 10^6 cells were surface stained for 30 min with antibodies for PerCP-Cy5.5 conjugated CD11c, PE-conjugated CD19, APC-conjugated F4.80, and FITC-conjugated CD45 (all antibodies were purchased from eBiosciences) for the detection of the different antigen-presenting cells. For the detection of T cell subsets, 1x10^6 cells were initially surface stained for 30 min with FITC-conjugated CD8α, PE-conjugated CD4, and APC-conjugated TCRαβ (ebiosciences). Specifically for the differentiation of memory vs. naïve T cells, the cells were stained with FITC-conjugated CD62l, PE-conjugated CD44, PerCP-Cy5.5-conjugated CD4, and APC-conjugated CD8α (ebiosciences). Analysis was performed using an Accuri C6 flow cytometer (Accuri Cytometers).

Pre-processing of fecal samples for separation of viruses and bacteria

Fecal samples from three different time points were included to investigate GM changes over time: arrival at our housing facility, 1 week after 2nd FVT, and at termination of the study, which represented in total 144 fecal samples. Separation of viruses and bacteria from fecal samples generated a fecal pellet and fecal supernatant by centrifugation and 0.45 µm filtering as described previously[41], however, the volume of fecal homogenate was adjusted to 5 mL SM buffer.

Bacterial DNA extraction, sequencing, and pre-processing of raw data

The DNeasy PowerSoil Pro Kit (Qiagen) was used to extract bacterial DNA from the fecal pellet by following the instructions of the manufacturer. The final purified DNA was stored at -80ºC, and the DNA concentration was determined using Qubit HS Assay Kit (Invitrogen) on the Qubit 4 Fluorometric Quantification device (Invitrogen). The bacterial community composition was determined by Illumina NextSeq-based high-throughput sequencing (HTS) of the 16S rRNA gene V3-region, as previously described[41]. Quality control of reads, de-replicating, purging from chimeric reads and constructing zOTU was conducted with the UNOISE pipeline and taxonomically assigned with Sintax. Taxonomical assignments were obtained using the EZtaxon for 16S rRNA gene database. Code describing this pipeline can be accessed in github.com/jcame/Fastq_2_zOTUtable. The average sequencing depth after quality control (Accession: PRJEB58786, available at ENA) for the fecal 16S rRNA gene amplicons was 67,454 reads (min. 12,790 reads and max. 295,746 reads).

Viral RNA/DNA extraction, sequencing and pre-processing of raw data

The sterile filtered fecal supernatant was concentrated using centrifugal filters Centrisart with a filter cut-off at 100 kDA (Sartorius) by centrifugation centrifuged at 1,500 x g at 4ºC (dx.doi.org/10.17504/protocols.io.b2qaqdse). The viral DNA/RNA was extracted from the fecal supernatants with Viral RNA mini kit (Qiagen) as previously described[41]. Reverse transcription was performed with SuperScript VILO Master mix by following the instructions of the manufacturer and subsequently cleaned with DNeasy blood and tissue kit (Qiagen) by only following step 3-8. In brief, the DNA/cDNA samples were mixed with ethanol, bound to the silica filter, washed two times, and eluted with 40 µL elution buffer. Multiple displacement amplification (MDA, to include ssDNA viruses) using GenomiPhi V3 DNA amplification kit (Cytiva) and sequencing library preparation using Nextera XT kit was performed as previously described[41], and sent for sequencing using the NovaSeq platform (NovoGene). The average sequencing depth of raw reads (Accession: PRJEB58786, available at ENA) for the fecal viral metagenome was 13,145,283 reads (min. 693,882 reads and max. 142,821,858 reads. The raw reads were trimmed from adaptors and the high-quality sequences (>95% quality) using Trimmomatic v0.35 with a minimum size of 50nt were retained for further analysis. High-quality reads were de-replicated and checked for the presence of PhiX control using BBMap (bbduk.sh) (https://www.osti.gov/servlets/purl/1241166). Virus-like particle-derived DNA sequences were subjected to within-sample de-novo assembly-only using Spades v3.13.1 and the contigs with a minimum length of 2,200 nt, were retained. Contigs generated from all samples were pooled and de-replicated at 90% identity using BBMap (dedupe.sh). Prediction of viral contigs/genomes was carried out using VirSorter2 ("full" categories | dsDNAphage, ssDNA, RNA, Lavidaviridae, NCLDV | viralquality ≥ 0.66), vibrant (High-quality | Complete), and checkv (High-quality | Complete). Taxonomy was inferred by blasting viral ORF against viral orthologous groups (https://vogdb.org) and the Lowest Common Ancestor (LCA) for every contig was estimated based on a minimum e-value of $10e^{-5}$. Phage-host prediction was determined by blasting (85% identity) CRISPR spacers and tRNAs predicted from >150,000 gut species-level genome bins (SGBs) Following assembly, quality control, and annotations, reads from all samples were mapped against the viral (high-quality) contigs (vOTUs) using the bowtie2 and a contingency table of reads per Kbp of contig sequence per million reads sample (RPKM) was generated, here defined as vOTU-table (viral contigs). Code describing this pipeline can be accessed in github.com/jcame/virome_analysis-FOOD.

Bioinformatic analysis and statistics

Initially, the dataset was purged for zOTU's/viral contigs, which were detected in less than 5% of the samples, but the resulting dataset still maintained 99.8% of the total reads. Cumulative sum scaling (CSS) normalization was performed using the R software using the metagenomeSeq package. R version 4.3.0 was used for subsequent analysis and presentation of data. The main packages used were phyloseq, vegan, deseq2, ampvis2, ggpubr, and ggplot2. A-diversity analysis was based on raw read counts and statistics were based on ANOVA. B-diversity was represented by Bray-Curtis dissimilarity and statistics were based on PERMANOVA The Kruskal Wallis test was adopted for analysis of the differentially abundant viral contigs (vOTUs) and their predicted bacterial hosts in heat map. Cytokine levels, immune cell levels, eWAT, bodyweight, OGTT, and histology data were analyzed in R using linear regression models (similar to ANOVA) with either the obese or lean control mice as references.

Acknowledgments

We thank the animal caretakers Helene Farlov and Mette Nelander at Section of Experimental Animal Models (University of Copenhagen, Denmark) for taking care of the animals during the study and assisting with the animal handling.

Disclosure statement

All authors declare no conflicts of interest is associated with participation and contribution to this work.

Funding

This work was supported by the Lundbeck Foundation under Grant R324-2019-1880, and the Novo Nordisk Foundation under Grant NNF-20OC0063874.

Author Contributions

TSR and DSN conceived the research idea and designed the study; TSR and SBL, performed the experiments; TSR, SBL, XM, LSFZ, AB, SA, JLCM, CHFH, KA, and AKH performed laboratory and data analysis; XM and TSR wrote the first draft of the manuscript. All authors critically revised and approved the final version of the manuscript.

Data availability statement

All data associated with this study are present in the paper or the Supplementary Materials. All 529 sequencing datasets are available in the ENA database under accession number PRJEB58786.

References

1. Afshin, A. *et al.* Health effects of overweight and obesity in 195 countries over 25 years. *New England Journal of Medicine* **377**, 13–27 (2017).

2. Thaiss, C. A. *et al.* Persistent microbiome alterations modulate the rate of post-dieting weight regain. *Nature* **540**, 544–551 (2016).

3. Leitner, D. R. *et al.* Obesity and type 2 diabetes: Two diseases with a need for combined treatment strategies - EASO can lead the way. *Obes Facts* **10**, 483–492 (2017).

4. Wilcox, M. H., McGovern, B. H. & Hecht, G. A. The efficacy and safety of fecal microbiota transplant for recurrent *Clostridium difficile* infection: current understanding and gap analysis. *Open Forum Infect Dis* **7**, (2020).

5. Park, R., Umar, S. & Kasi, A. Immunotherapy in colorectal cancer: Potential of fecal transplant and microbiota-augmented clinical trials. *Curr Colorectal Cancer Rep* **16**, 81–88 (2020).

6. Brunse, A. *et al.* Fecal filtrate transplantation protects against necrotizing enterocolitis. *ISME J* **16**, 686–694 (2022).

7. Brunse, A. *et al.* Effect of fecal microbiota transplantation route of administration on gut colonization and host response in preterm pigs. *ISME J* **13**, 720–733 (2019).

8. Lahtinen, P. *et al.* Effectiveness of fecal microbiota transplantation for weight loss in patients with obesity undergoing bariatric surgery. *JAMA Netw Open* **5**, e2247226 (2022).

9. Allegretti, J. R. *et al.* Effects of fecal microbiota transplantation with oral capsules in obese patients. *Clinical Gastroenterology and Hepatology* **18**, 855-863.e2 (2020).

10. Yu, E. W. *et al.* Fecal microbiota transplantation for the improvement of metabolism in obesity: The FMT-TRIM double-blind placebo-controlled pilot trial. *PLoS Med* **17**, e1003051 (2020).

11. Mullish, B. H. *et al.* The use of faecal microbiota transplant as treatment for recurrent or refractory *Clostridium difficile* infection and other potential indications: joint British Society of Gastroenterology (BSG) and Healthcare Infection Society (HIS) guidelines. *Gut* **67**, 1920–1941 (2018).

12. U.S. Food & Drug Administration. Important safety alert regarding use of fecal microbiota for transplantation and risk of serious adverse reactions due to transmission of multi-drug resistant organisms. https://www.fda.gov/vaccines-blood-biologics/safety-availability-biologics/important-safety-alert-regarding-use-fecal-microbiota-transplantation-and-risk-serious-adverse (2019).

13. U.S. Food & Drug Administration. Safety alert regarding use of fecal microbiota for transplantation and additional safety protections pertaining to monkeypox virus. (2022).

14. U.S. Food & Drug Administration. Safety alert regarding use of fecal microbiota for transplantation and risk of serious adverse events likely due to transmission of pathogenic organisms. https://www.fda.gov/vaccines-blood-biologics/safety-availability-biologics/safety-alert-regarding-use-fecal-microbiota-transplantation-and-risk-serious-adverse-events-likely (2020).

15. Marotz, C. A. & Zarrinpar, A. Treating obesity and metabolic syndrome with fecal microbiota transplantation. *Yale J Biol Med* **89**, 383–388 (2016).

16. Liang, G. *et al.* The stepwise assembly of the neonatal virome is modulated by breastfeeding. *Nature* **581**, 470–474 (2020).

17. Lim, E. S. *et al.* Early life dynamics of the human gut virome and bacterial microbiome in infants. *Nat Med* **21**, 1228–1234 (2015).

18. Rasmussen, T. S. *et al.* Bacteriophage-mediated manipulation of the gut microbiome - promises and presents limitations. *FEMS Microbiol Rev* **44**, 507–521 (2020).

19. Cao, Z. *et al.* The gut virome: A new microbiome component in health and disease. *EBioMedicine* **81**, 104113 (2022).

20. Shah, S. A. *et al.* Expanding known viral diversity in the healthy infant gut. *Nat Microbiol* **8**, 986–998 (2023).

21. Doorbar, J., Egawa, N., Griffin, H., Kranjec, C. & Murakami, I. Human papillomavirus molecular biology and disease association. *Rev Med Virol* **25**, 2–23 (2015).

22. Ott, S. J. *et al.* Efficacy of sterile fecal filtrate transfer for treating patients with *Clostridium difficile* infection. *Gastroenterology* **152**, 799-811.e7 (2017).

23. Kao, D. H., Roach, B., Walter, J., Lobenberg, R. & Wong, K. Effect of lyophilized sterile fecal filtrate vs lyophilized donor stool on recurrent *Clostridium difficile* infection (rCDI): Prelimenary results from a randomized, double-blind pilot study. *J Can Assoc Gastroenterol* **2**, 101–102 (2019).

24. Rasmussen, T. S. *et al.* Faecal virome transplantation decreases symptoms of type 2 diabetes and obesity in a murine model. *Gut* **69**, 2122–2130 (2020).

25. Borin, J. M. *et al.* Fecal virome transplantation is sufficient to alter fecal microbiota and drive lean and obese body phenotypes in mice. *bioRxiv* (2023) doi:10.1101/2023.02.03.527064.

26. Rasmussen, T. S. *et al.* Overcoming donor variability and risks associated with fecal microbiota transplants through bacteriophage-mediated treatments. *bioRxiv* (2023) doi:10.1101/2023.03.17.532897.

27. Adamberg, S., Rasmussen, T. S., Larsen, S. B., Nielsen, D. S. & Adamberg, K. Reproducible chemostat cultures to eliminate eukaryotic viruses from fecal transplant material. *bioRxiv* (2023) doi:10.1101/2023.03.15.529189.

28. Rey, F. A. & Lok, S.-M. Common features of enveloped viruses and implications for immunogen design for next-generation vaccines. *Cell* **172**, 1319–1334 (2018).

29. Koonin, E. V., Dolja, V. V. & Krupovic, M. Origins and evolution of viruses of eukaryotes: The ultimate modularity. *Virology* vols 479–480 2–25 Preprint at https://doi.org/10.1016/j.virol.2015.02.039 (2015).

30. Sausset, R., Petit, M. A., Gaboriau-Routhiau, V. & De Paepe, M. New insights into intestinal phages. *Mucosal Immunol* **13**, 205–215 (2020).

31. WHO Health Product Policy and Standards Team. Guidelines on viral inactivation and removal procedures intended to assure the viral safety of human blood plasma products. WHO-TRS924-Annex4-1-82 https://www.who.int/publications/m/item/WHO-TRS924-Annex4 (2004).

32. Horowitz, B. *et al.* Solvent/detergent-treated plasma: a virus-inactivated substitute for fresh frozen plasma. *Blood* **79**, 826–31 (1992).

33. Kapuscinski, J. & Darzynkiewicz, Z. Interactions of pyronin Y(G) with nucleic acids. *Cytometry* **8**, 129–37 (1987).

34. Darzynkiewicz, Z., Kapuscinski, J., Carter, S. P., Schmid, F. A. & Melamed, M. R. Cytostatic and cytotoxic properties of pyronin Y: relation to mitochondrial localization of the dye and its interaction with RNA. *Cancer Res* **46**, 5760–6 (1986).

35. Rao, K. *et al.* The systemic inflammatory response to *Clostridium difficile* infection. *PLoS One* **9**, e92578 (2014).

36. Fraulob, J. C., Ogg-Diamantino, R., Fernandes-Santos, C., Aguila, M. B. & Mandarim-de-Lacerda, C. A. A mouse model of metabolic syndrome: Insulin resistance, fatty liver and non-alcoholic fatty pancreas disease (NAFPD) in C57BL/6 mice fed a high fat diet. *J Clin Biochem Nutr* **46**, 212–223 (2010).

37. Hui, Y. *et al.* Donor-dependent fecal microbiota transplantation efficacy against necrotizing enterocolitis in preterm pigs. *NPJ Biofilms Microbiomes* **8**, (2022).

38. Lundberg, R., Bahl, M. I., Licht, T. R., Toft, M. F. & Hansen, A. K. Microbiota composition of simultaneously colonized mice housed under either a gnotobiotic isolator or individually ventilated cage regime. *Sci Rep* **7**, 1–11 (2017).

39. Rasmussen, T. S. *et al.* Inter-vendor variance of enteric eukaryotic DNA viruses in specific pathogen free C57BL/6N mice. *Res Vet Sci* **136**, 1–5 (2021).

40. Ericsson, A. C. *et al.* Effects of vendor and genetic background on the composition of the fecal microbiota of inbred mice. *PLoS One* **10**, 1–19 (2015).

41. Rasmussen, T. S. *et al.* Mouse vendor influence on the bacterial and viral gut composition exceeds the effect of diet. *Viruses* **11**, (2019).

42. Santiago-Rodriguez, T. M. *et al.* Chemostat culture systems support diverse bacteriophage communities from human feces. *Microbiome* **3**, 58 (2015).

43. Powell, E. E., Wong, V. W.-S. & Rinella, M. Non-alcoholic fatty liver disease. *The Lancet* **397**, 2212–2224 (2021).

44. Weisberg, S. P. *et al.* Obesity is associated with macrophage accumulation in adipose tissue. *J Clin Invest* **112**, 1796–1808 (2003).

45. Nishimura, S. *et al.* CD8+ effector T cells contribute to macrophage recruitment and adipose tissue inflammation in obesity. *Nat Med* **15**, 914–920 (2009).

46. Sutti, S. *et al.* CX3CR1-expressing inflammatory dendritic cells contribute to the progression of steatohepatitis. *Clin Sci* **129**, 797–808 (2015).

47. Guarner, V. & Rubio-Ruiz, M. E. Low-grade systemic inflammation connects aging, metabolic syndrome and cardiovascular disease. *Interdiscip Top Gerontol* **40**, 99–106 (2015).

48. Mansyur, M. A., Bakri, S., Patellongi, I. J. & Rahman, I. A. The association between metabolic syndrome components, low-grade systemic inflammation and insulin resistance in non-diabetic Indonesian adolescent male. *Clin Nutr ESPEN* **35**, 69–74 (2020).

49. Qin, C. C., Liu, Y. N., Hu, Y., Yang, Y. & Chen, Z. Macrophage inflammatory protein-2 as mediator of inflammation in acute liver injury. *World J Gastroenterol* **23**, 3043–3052 (2017).

50. Kakino, S. *et al.* Pivotal role of TNF-α in the development and progression of nonalcoholic fatty liver disease in a murine model. *Hormone and Metabolic Research* **50**, 80–87 (2018).

51. Stanley, T. L. *et al.* TNF-α antagonism with etanercept decreases glucose and increases the proportion of high molecular weight adiponectin in obese subjects with features of the metabolic syndrome. *J Clin Endocrinol Metab* **96**, E146–E150 (2011).

52. Quinn, le B. S., Anderson, B. G., Conner, J. D., Pistilli, E. E. & Wolden-Hanson, T. Overexpression of interleukin-15 in mice promotes resistance to diet-induced obesity, increased insulin sensitivity, and markers of oxidative skeletal muscle metabolism. *Int J Interferon Cytokine Mediat Res* **3**, 29–42 (2011).

53. Guo, W. L. *et al.* Hypoglycemic and hypolipidemic mechanism of organic chromium derived from chelation of Grifola frondosa polysaccharide-chromium (III) and its modulation of intestinal microflora in high fat-diet and STZ-induced diabetic mice. *Int J Biol Macromol* **145**, 1208–1218 (2020).

54. van Muijlwijk, G. H. *et al.* Identification of *Allobaculum mucolyticum* as a novel human intestinal mucin degrader. *Gut Microbes* **13**, (2021).

55. Cox, L. M. *et al.* Altering the intestinal microbiota during a critical developmental window has lasting metabolic consequences. *Cell* **158**, 705–721 (2014).

56. Scheithauer, T. P. M. *et al.* Gut Microbiota as a Trigger for Metabolic Inflammation in Obesity and Type 2 Diabetes. *Front Immunol* **11**, 571731 (2020).

57. Duarte, S. M. B. *et al.* Gut microbiome composition in lean patients with NASH is associated with liver damage independent of caloric intake: A prospective pilot study. *Nutrition, Metabolism and Cardiovascular Diseases* **28**, 369–384 (2018).

58. Raman, M. *et al.* Fecal microbiome and volatile organic compound metabolome in obese humans with nonalcoholic fatty liver disease. *Clinical Gastroenterology and Hepatology* **11**, 868-875.e3 (2013).

59. Reynolds, R. *et al.* A systematic review of chronic disease management interventions in primary care. *BMC Fam Pract* **19**, (2018).

60. Prince, A. M., Horowitz, B. & Brotman, B. Sterilisation of hepatitis and HTLV-III viruses by exposure to tri(n-butyl)phosphate and sodium cholate. *Lancet* **1**, 706–10 (1986).

61. Remy, M. M. *et al.* Effective chemical virus inactivation of patient serum compatible with accurate serodiagnosis of infections. *Clin Microbiol Infect* **25**, 907.e7-907.e12 (2019).

62. Trescec, A., Simić, M., Branović, K., Gebauer, B. & Benko, B. Removal of detergent and solvent from solvent-detergent-treated immunoglobulins. *J Chromatogr A* **852**, 87–91 (1999).

63. Pettersson, U. S., Waldén, T. B., Carlsson, P.-O., Jansson, L. & Phillipson, M. Female mice are protected against high-fat diet induced metabolic syndrome and increase the regulatory T cell population in adipose tissue. *PLoS One* **7**, e46057 (2012).

64. Tougaard, P. *et al.* TL1A regulates adipose-resident innate lymphoid immune responses and enables diet-induced obesity in mice. *Int J Obes* **44**, 1062–1074 (2020).

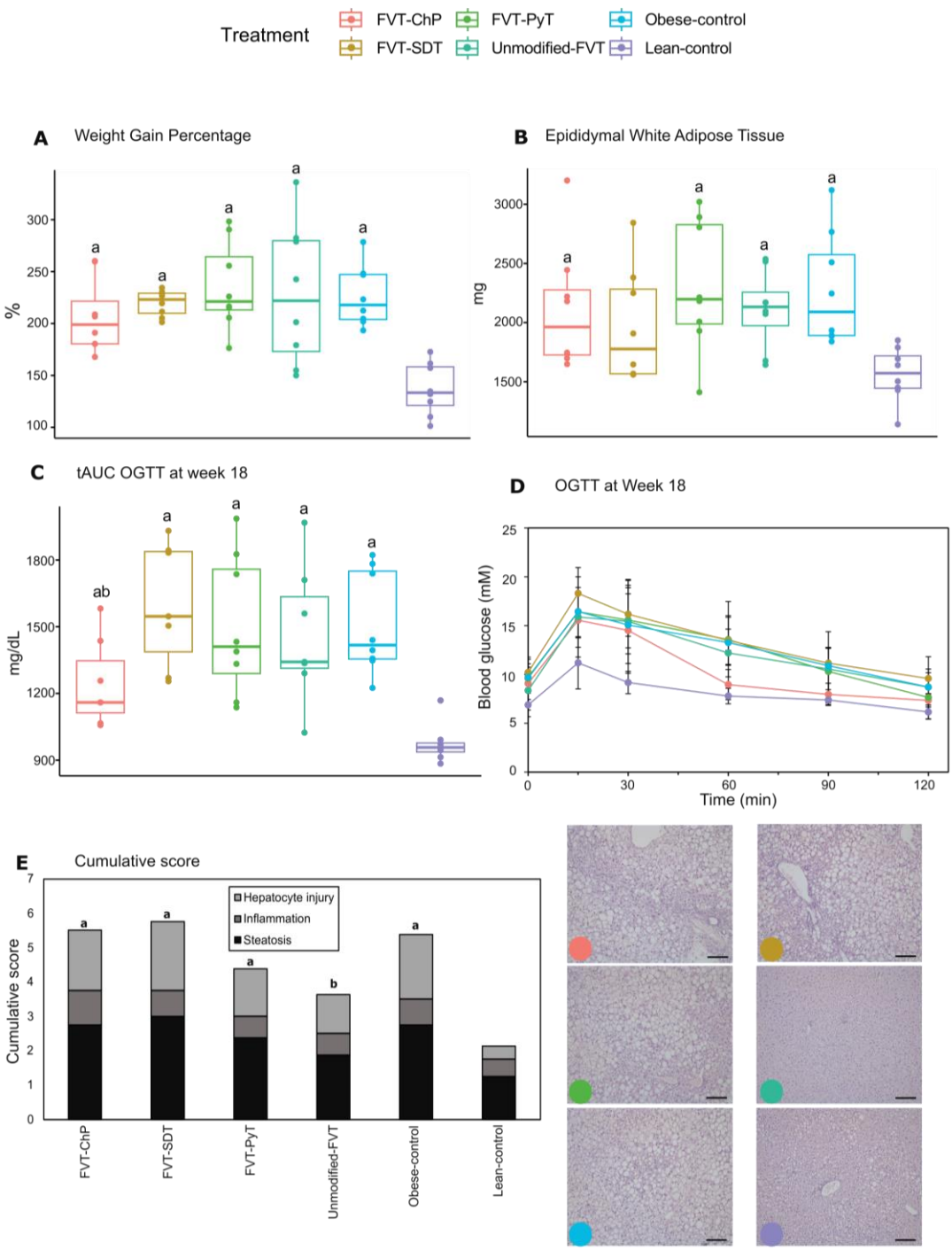

Fig. 1: Overview of mouse phenotypic characteristics after being treated with modified and unmodified FVTs. A) Weight gain percentage, B) measure of epididymal white adipose tissue size (eWAT). C) Total area under the curve (tAUC) of the D) oral glucose tolerance test (OGTT) measured at termination of the study (23 weeks old). E) Cumulative score and representative histology images related to liver tissue pathology. Significant changes ($p < 0.05$) when comparing the FVT treatments with the lean (a) and obese control mice (b) are marked accordingly. Scale in histology images = 300 µm.

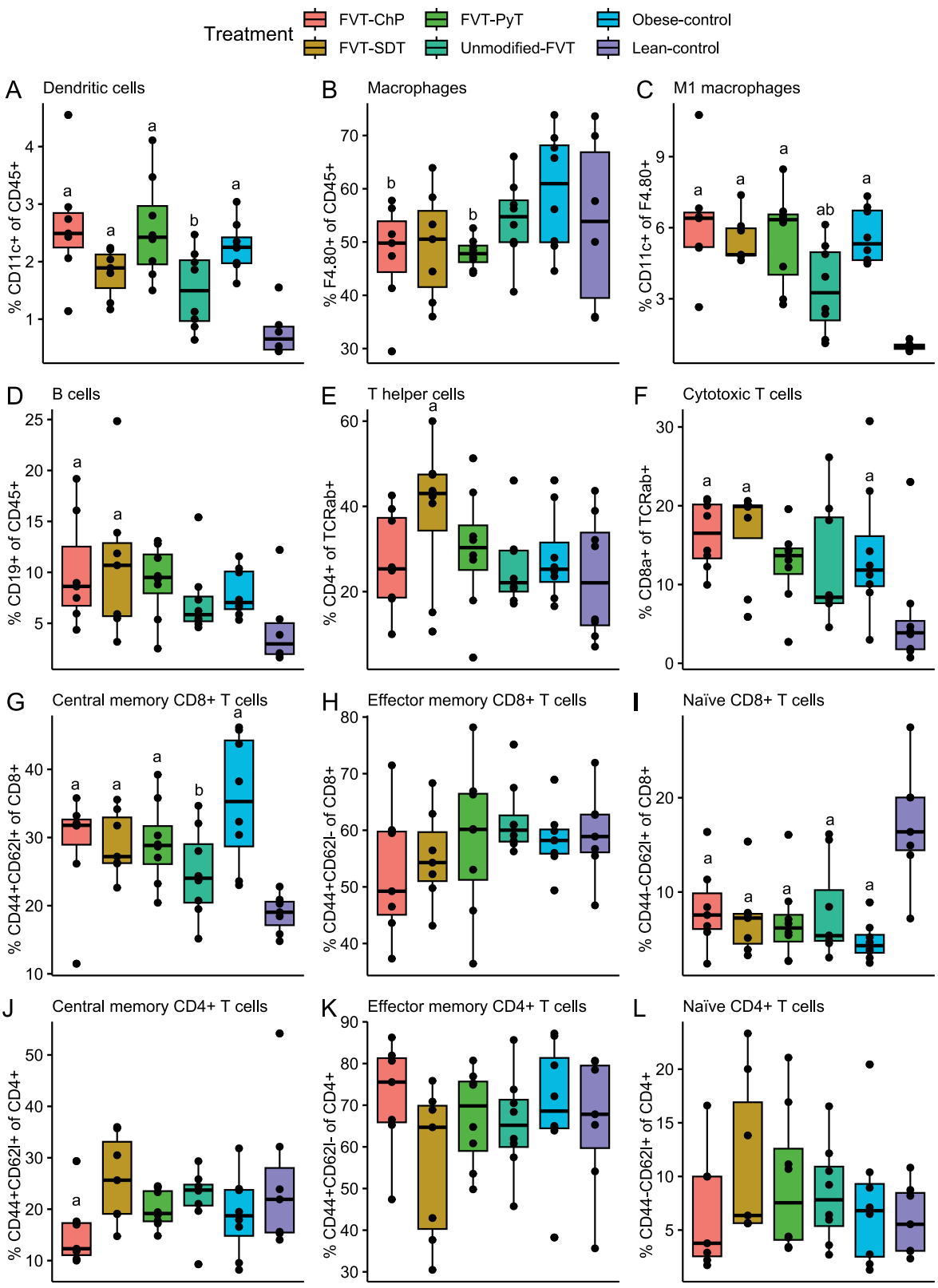

Fig. 2: Immune cell count in adipose tissue at study termination (23 weeks old). A) to L) are showing the overall fluorescence-activated cell sorter (FACS) profile in the mouse adipose tissue. Significant changes ($p < 0.05$) when comparing the FVT treatments with the lean (a) and obese control mice (b) are marked accordingly.

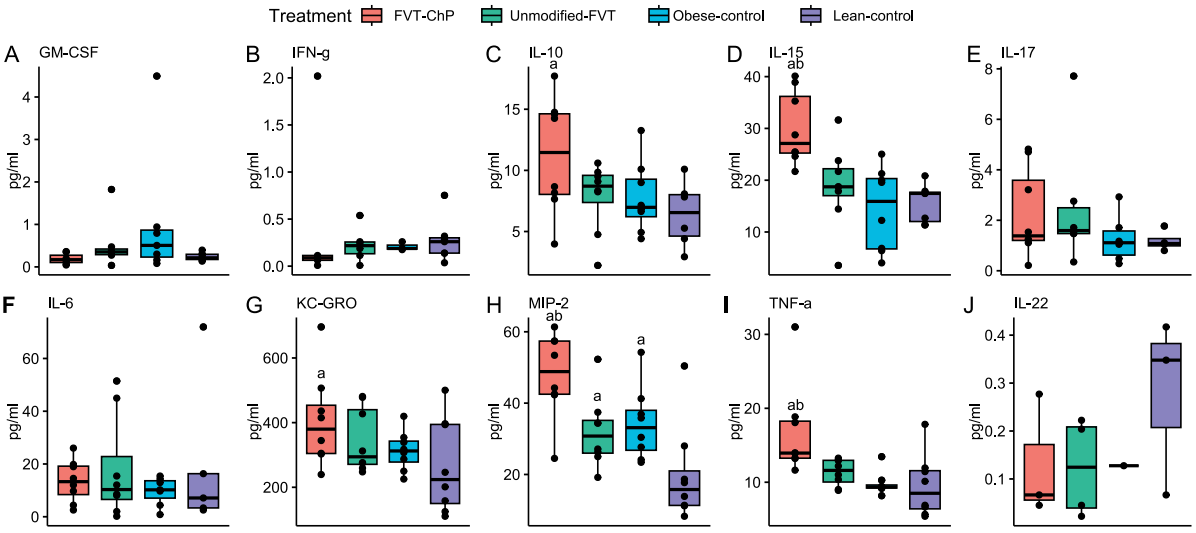

Fig. 3: Cytokine profiles of blood serum sampled at termination (23 weeks old). A) to J) are showing the overall cytokine profile in the mouse blood serum of mice treated with FVT-ChP, unmodified FVT, and the two dietary control groups. Significant changes ($p < 0.05$) when comparing the FVT treatments with the lean (a) and obese control mice (b) are marked accordingly.

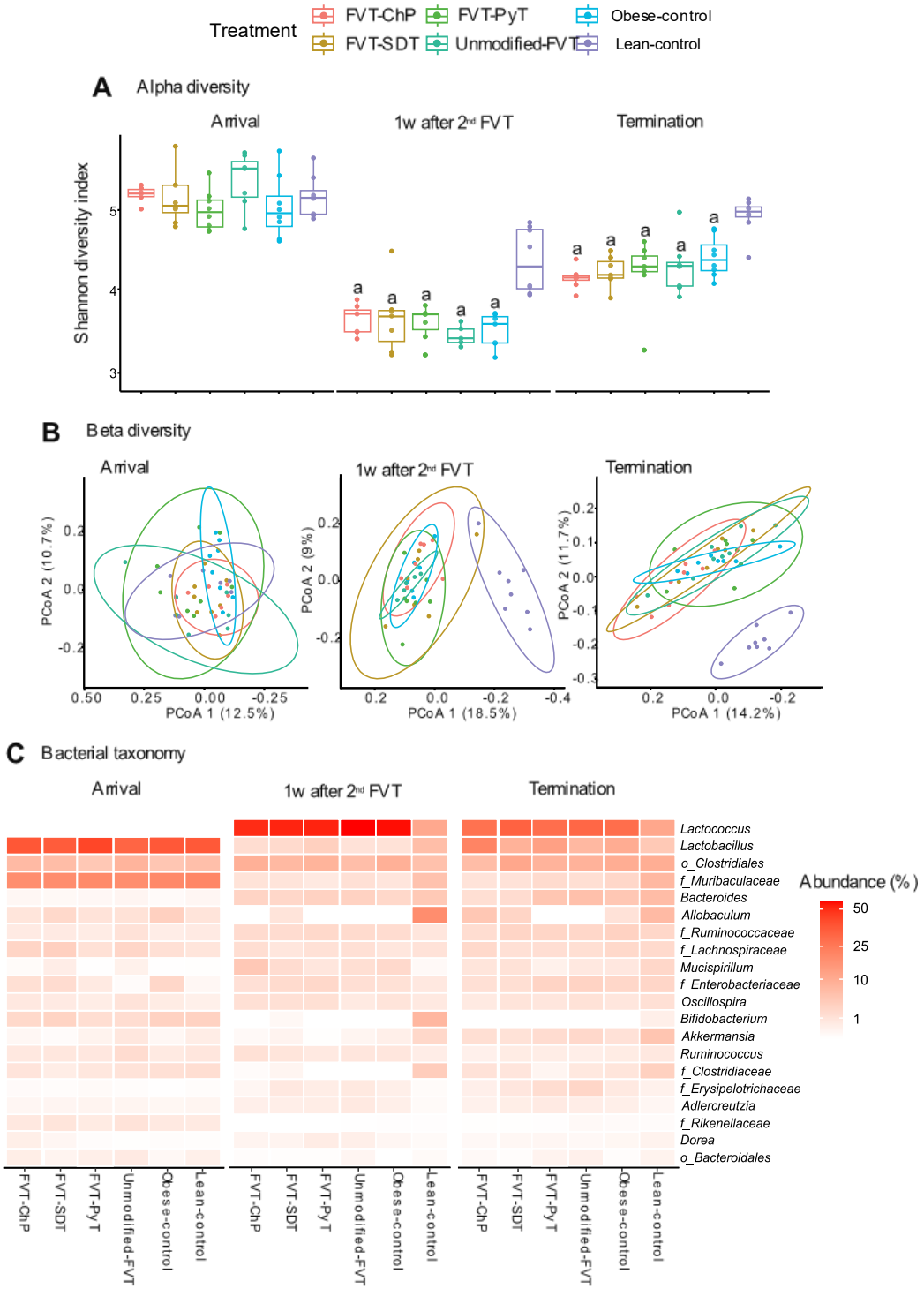

Fig. 4: Bacteriome analysis based on 16S rRNA gene amplicon sequencing at three time points: at arrival before diet intervention (5 weeks old), one week after 2nd FVT (14 weeks old), and study termination (23 weeks old). A) The general bacterial diversity (Shannon diversity index), B) PCoA plot of the bacterial composition (Bray-Curtis dissimilarity), and C) heatmap representing the relative abundance of dominating bacterial taxa. Significant changes ($p < 0.05$) when comparing the FVT treatments with the lean (a) and obese control mice (b) are marked accordingly.

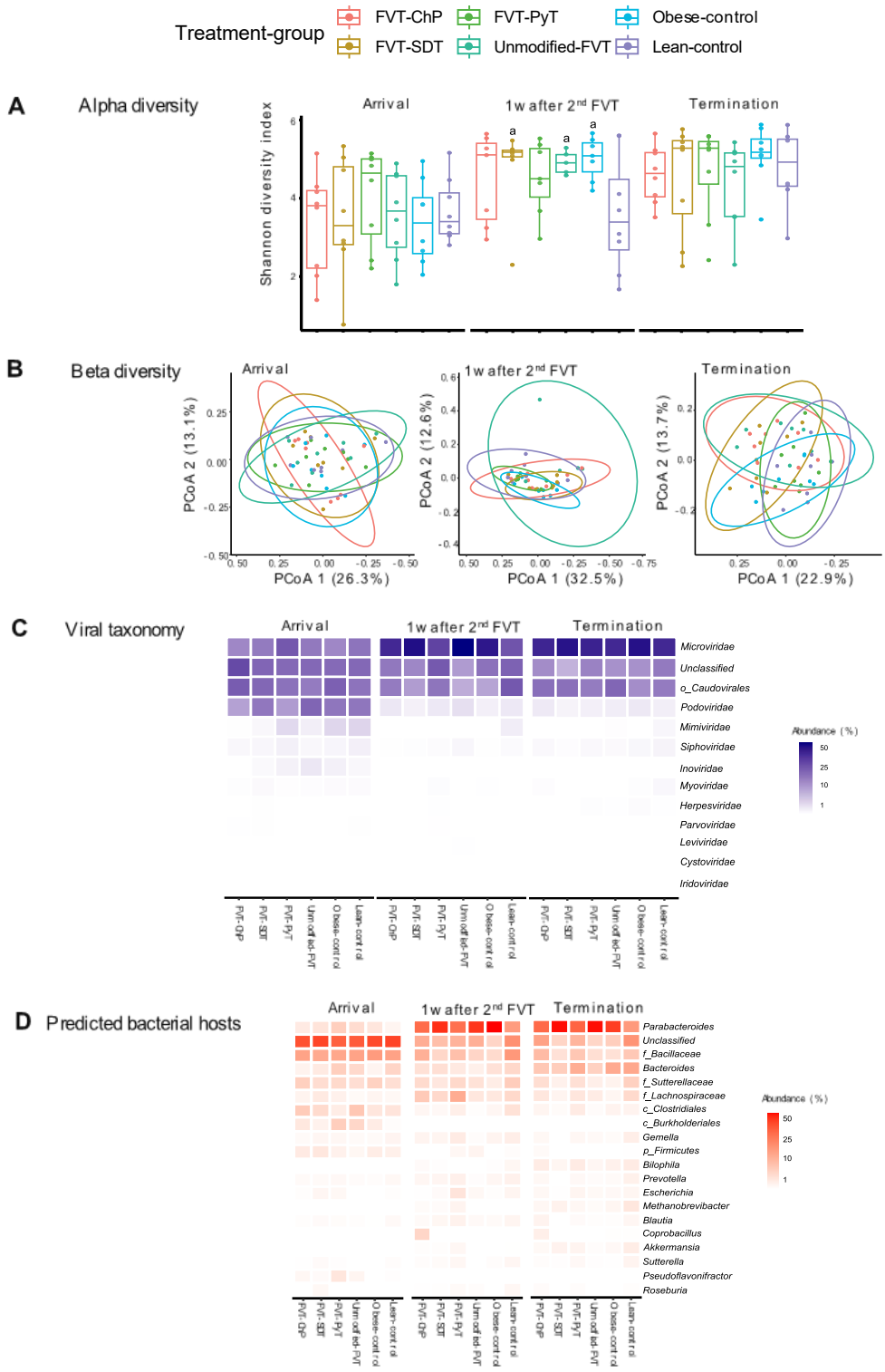

Fig. 5: Metavirome analysis based on whole-genome sequencing of viral-like entities at three time points: at arrival before diet intervention (5 weeks old), one week after 2nd FVT (14 weeks old), and study termination (23 weeks old). A) The general viral diversity (Shannon diversity index), B) PCoA plot of the viral composition (Bray-Curtis dissimilarity), and C) heatmap representing the relative abundance of dominating viral taxa. Significant changes ($p < 0.05$) when comparing the FVT treatments with the lean (a) and obese control mice (b) are marked accordingly.

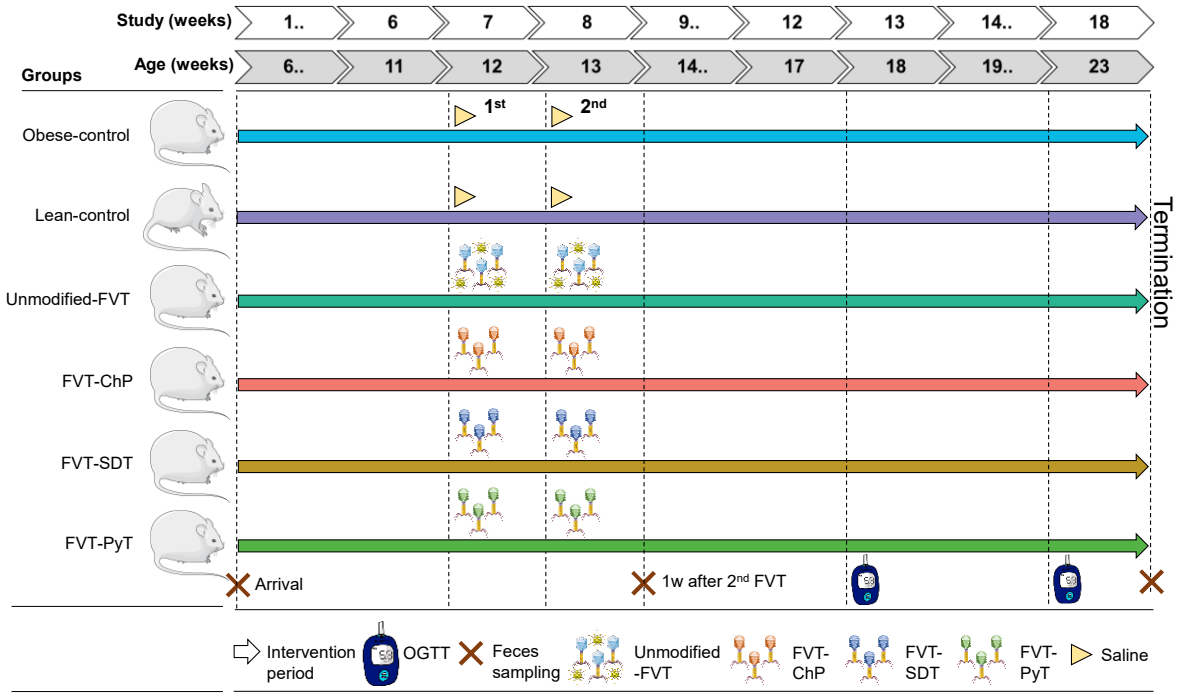

Fig. 6: Overview of the animal study design. Forty-eight male C57BL/6NTac mice (5 weeks old) were divided into six groups. The mice were fed with either high-fat diet or low-fat diet. The mice were treated with differently modified fecal virome transplantations (FVTs), after 6 and 7 weeks on a high-fat diet. The treatments represented an unmodified FVT (containing all viruses but no bacteria), chemostat propagated fecal virome depleted for eukaryotic viruses by dilution (FVT-ChP), solvent-detergent treated FVT to inactivate enveloped viruses (FVT-SDT), and pyronin Y treated FVT to inactive RNA viruses, and a saline solution for the obese and lean control. Oral glucose tolerance tests (OGTT) were measured twice (18 and 23 weeks old). The crosses mark the timepoint of feces samples that were used for gut microbiome analysis.